HOFMANN, K. A. & KIRMREUTHER, H. (1909). *Ber. dtsch. chem. Ges.* **42**, 4856.
International Tables for X-ray Crystallography (1952). Vol. I, p. 319. Birmingham: Kynoch Press.
KAY, M. I. & BEHRENDT, D. R. (1963). *Acta Cryst.* **16**, 157.
SHARP, D. W. A. & SHEPPARD, N. (1957). *J. Chem. Soc.* 674.
STORA, C. (1958). *C. R. Acad. Sci. Paris.* **246**, 1693.
SUNDARALINGAM, M. & JENSEN, L. H. (1963). *J. Amer. Chem. Soc.* **85**, 3302.
VIERVOLL, H. & ØGRIM, O. (1949). *Acta Cryst.* **2**, 277.

Acta Cryst. (1965). **18**, 443

The Surface Re-Orientation Caused by Unidirectional Abrasion on Polycrystalline Antimony

BY M. F. STROUD AND H. WILMAN

Applied Physics and Chemistry of Surfaces Laboratory, Department of Chemical Engineering and Chemical Technology, Imperial College, London, S.W. 7, England

(*Received* 24 *March* 1964)

Electron diffraction is used to examine the surface re-orientation produced on a polycrystalline antimony surface by unidirectional abrasion. The immediate surface region is randomly disoriented, but at a few hundred to ~ 10,000 Å depth the main feature of the re-orientation is a large azimuthal spread about a [111] trigonal axis which is forwardly inclined from the outward specimen normal towards the direction in which the abrasive particles travel. This azimuthal range extends to at least ± 30° from the mean, which is such that a [1$\bar{1}$0] or [$\bar{1}$10] direction is normal to the abrasion direction; and it may possibly be up to ±60°, although it is suggested that the latter may be due to pseudo-octahedral twinning (relative to the f.c. rhombohedral pseudo-cubic cell). This abrasion texture is completely analogous, in respect of type of orientation axis and sense of its inclination, to that produced by abrasion on zinc and cadmium. However, additional evidence leads to the conclusion that the above structure is a secondary, though prominent, modification of an initially produced, backwardly inclined (110) (f.c. rhombohedral axes) orientation, analogous to that observed in the case of the f.c. cubic metals.

1. Introduction

Recent results from this laboratory (see Goddard, Harker & Wilman, 1962; King & Wilman, 1961, 1962; Dobson & Wilman, 1962*a*, *b*) have shown the nature of the preferred orientation of the surface regions of metals and inorganic non-metallic materials abraded unidirectionally on emery papers. In general, materials of the same structure type show the same type of orientation, and this is closely similar in type and azimuthal preference to the rolling texture.

In all the materials examined, except zinc and cadmium, the orientation axis is inclined backward from the outward specimen normal, towards the direction from which the abrasive particles come; and the angle of tilt can be accounted for in relation to the coefficient of friction for the ploughing abrasive particles. However, in zinc and cadmium the orientation axis, [0001], is inclined forwards by 10 to 15° (Avient, 1961), in contrast to the backwardly tilted [0001] orientation observed for the hexagonal metals beryllium and magnesium (Scott & Wilman, 1958; Levin, 1960), but agreeing with the known rolling texture of zinc and cadmium (*cf.* Barrett, 1953).

In connection with our experiments on friction and wear during abrasion of antimony and bismuth (Stroud & Wilman, 1963), we have investigated by electron diffraction the surface structure (down to 2 microns depth) of antimony after unidirectional abrasion on 0000 emery paper wet with propyl alcohol, at a load of 1 kg. Our wear and friction results, and optical microscopy, showed that brittle fracture (cleavage) of the antimony surface regions occurs prominently during abrasion, and contributes much to the wear. Notwithstanding this, however, the results presented below show that much plastic flow also occurs and leads to a well-defined re-orientation of at least much of the surface region. The orientation developed is [0001] as for all the hexagonal metals, but this axis is tilted slightly forward, like that in zinc and cadmium. There is in addition marked azimuthal preference of the orientation, about this axis.

The crystal lattice of antimony is most simply described as rhombohedral with axial length $a_r = 4{\cdot}9762$ Å (at 25 °C), and rhombohedral angle $\alpha = 57° 6{\cdot}6'$ (Wyckoff, 1948), with two atoms per unit cell, in the positions uuu, $\bar{u}\bar{u}\bar{u}$, where $u = 0{\cdot}233$

(see also Cucka & Barrett, 1962). This lattice is expressed for present purposes as a face-centred rhombohedral lattice having $a_{fr} = 6{\cdot}222$ Å, $\alpha_{fr} = 87° 25{\cdot}4'$, which is face-centred pseudocubic and thus shows well the approximate equivalence of net planes whose Miller indices are permutations of any given three positive or negative integers. The coordinates of the pair of atoms associated with the lattice point at the origin are still as above, with the same value of u. For comparison with zinc and cadmium results, the antimony lattice is also described below in terms of hexagonal axes ($a=4{\cdot}308$, $c=11{\cdot}273$ Å; $c/a=2{\cdot}616$ at 25 °C) (Cucka & Barrett, 1962), the c axis being along the diagonal [111] of the rhombohedral cell, and the basal axes such that the rhombohedral axes a_r, b_r, c_r, are the vectors $[\frac{1}{3}\,\frac{2}{3}\,\frac{1}{3}]$, $[\frac{2}{3}\,\bar{\frac{1}{3}}\,\frac{1}{3}]$ and $[\bar{\frac{1}{3}}\,\bar{\frac{1}{3}}\,\frac{1}{3}]$ relative to the hexagonal axes. The structure factor S^2 relative to the hexagonal axes, is then:

$$S^2 = Sb^2 . 4\cos^2 2\pi(0{\cdot}233l) . \{1+2\cos 2\pi((h-k+l)/3)\}^2.$$

2. Experimental

The 'Specpure' antimony was obtained in rod form from Messrs. Johnson, Matthey & Co. Ltd. The specimen used in the present experiments was made by melting the antimony in a thoroughly cleaned porcelain crucible and quenching in water. This was then cut to a size of 1·75 cm × 1·25 cm bearing area and depth of 0·9 cm, using a fine jeweller's hacksaw. Etching showed the crystal grain diameter to be ~ 1 mm.

The bearing surface was then filed flat with a new, cleaned, grease-free 'smoothcut' steel file and abraded on successive grades of emery paper from 3 (particle diam. $D=150$ microns) down to 4/0 ($D=5$ microns). It was then metallographically polished by rubbing against a rotating disc covered with a 'Selvyt' cloth impregnated with a paste of 1–2 micron α-alumina suspended in benzene. By alternate polishing and etching (see below) the worked regions of the surface were gradually removed and electron diffraction was used to determine whether any initial structure, other than completely random disorientation of crystals, was present in the surface region.

The surface was then abraded unidirectionally on 4/0 emery paper, wet with propyl alcohol, for a distance of 500 cm under 1 kg load, each 25 cm stroke being made on fresh emery paper. If pick-up of abrasive emery occurs, then the electron diffraction patterns show presence of fine embedded diaspore (AlOOH) particles. The propyl alcohol served to avoid almost entirely such pick-up of abrasive emery and diaspore in the surface, and also reduced surface oxidation. After abrasion, the surface was washed in distilled water and immediately dehydrated by rinsing with acetone, and then transferred to the electron diffraction camera and evacuation started immediately.

The specimen, as prepared above, was then examined with the electron beam perpendicular to the abrasion direction, and also at various azimuths from this perpendicular setting, including the 'parallel' one where the beam is along the abrasion grooves. Similar experiments were made after successive layers of the abraded surface had been removed by etching, until the original undeformed random polycrystalline structure was observed. The type of camera used was as that described by Finch & Wilman (1937) but evacuated by oil diffusion pumps. A camera length of the order of 48 cm was used, and 50–60 kV accelerating potential difference.

Aqua regia was used to etch the antimony surface, this fast etchant removing the surface at about 800 Å per sec when freshly prepared. The mean depth of etch was calculated by determining the mass loss of the above abraded specimen after etching for a known time. The specimen was etched, washed in propyl alcohol and immediately dehydrated by rinsing with acetone, then dried thoroughly in a vacuum desiccator before being weighed on an Oertling semi-micro balance (accurate to 0·01 mg). This process was carried out after the diffraction experiments, at any given depth, had been completed, until the undeformed polycrystalline structure was reached.

3. Results

(a) *The initial grain orientation in the antimony specimen*

Fig. 1 shows the electron diffraction pattern of spotty rings characteristic of the initial texture of the antimony specimen surface prepared by polishing and etching away the worked layer as described in § 2. The relatively large crystal grains are seen to be randomly disoriented.

(b) *The electron diffraction patterns from the abraded surface and subsurface regions*

The following results were obtained with practically identical form in several repetitions of the experiments.

After unidirectional abrasion by sliding for 2000 cm on 4/0 emery paper (mean emery particle diameter 5 microns) under a load of 1 kg, the electron diffraction patterns of continuous rings showed that the abrasion had fragmented the surface metal and that at the immediate surface the fragments of antimony lattice were randomly oriented and mostly about 200 Å in diameter.

After etching away 1000–2000 Å thickness of metal, the surface then exposed yielded patterns such as Fig. 2(*a*) with the electron beam grazing the surface and normal to the abrasion direction, which was from right to left in Fig. 2(*a*); the mean crystal diameter in this region was again seen from Fig. 2(*a*) to be of the order of 200 Å. Figs. 2(*b*), (*c*) and (*d*) show the patterns obtained with the beam in azimuths 30°, 60° and 90° respectively from that of Fig. 2(*a*).

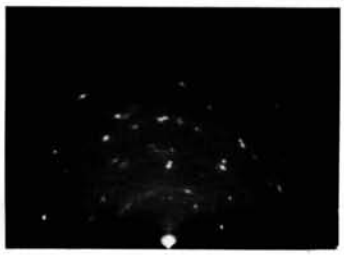

Fig. 1.

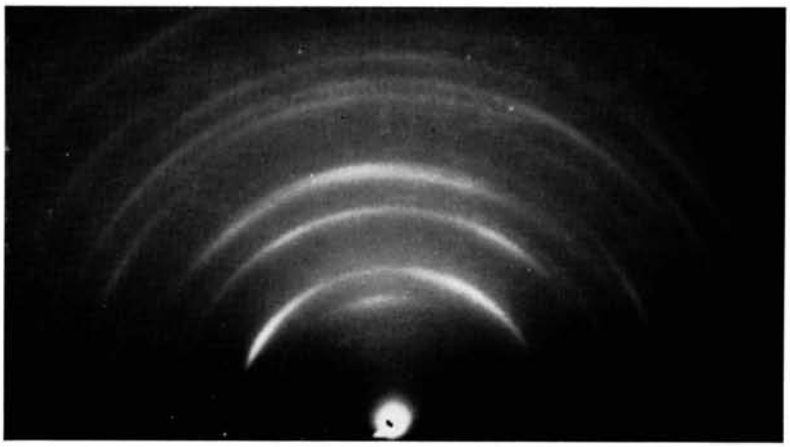

Fig. 2(*a*). (Enlarged 2·5 × linear).

Fig. 2(*b*).

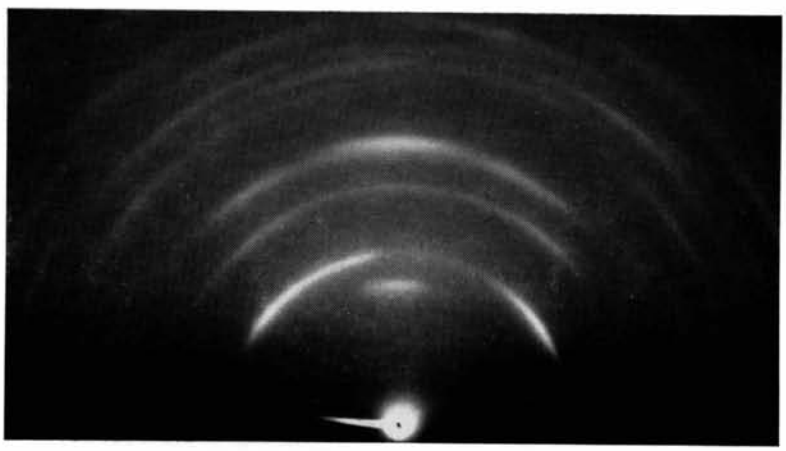

Fig. 3(*a*). (Enlarged 2·5 × linear).

Fig. 2(*c*).

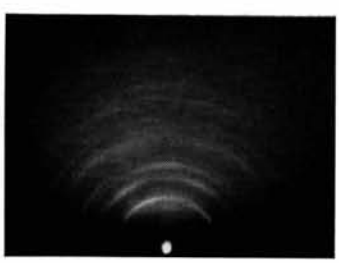

Fig. 2(*d*).

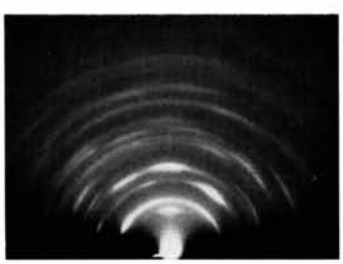

Fig. 3(*b*).

Fig. 1. E.D. pattern from cast and etched Sb; random orientation.
Fig. 2. As Fig. 1 but abraded right to left on 4/0 emery paper, wet with propylalcohol, at 1 kg load, then etched to ~2500 Å depth. Beam (*a*) ⊥, (*b*) at 60°, (*c*) at 30°, (*d*) ||, to the abrasion direction.
Fig. 3. As Fig. 2 but etched to ~7500 Å. Beam (*a*) ⊥, (*b*) at 60°, to abrasion direction.

[*To face p.* 444

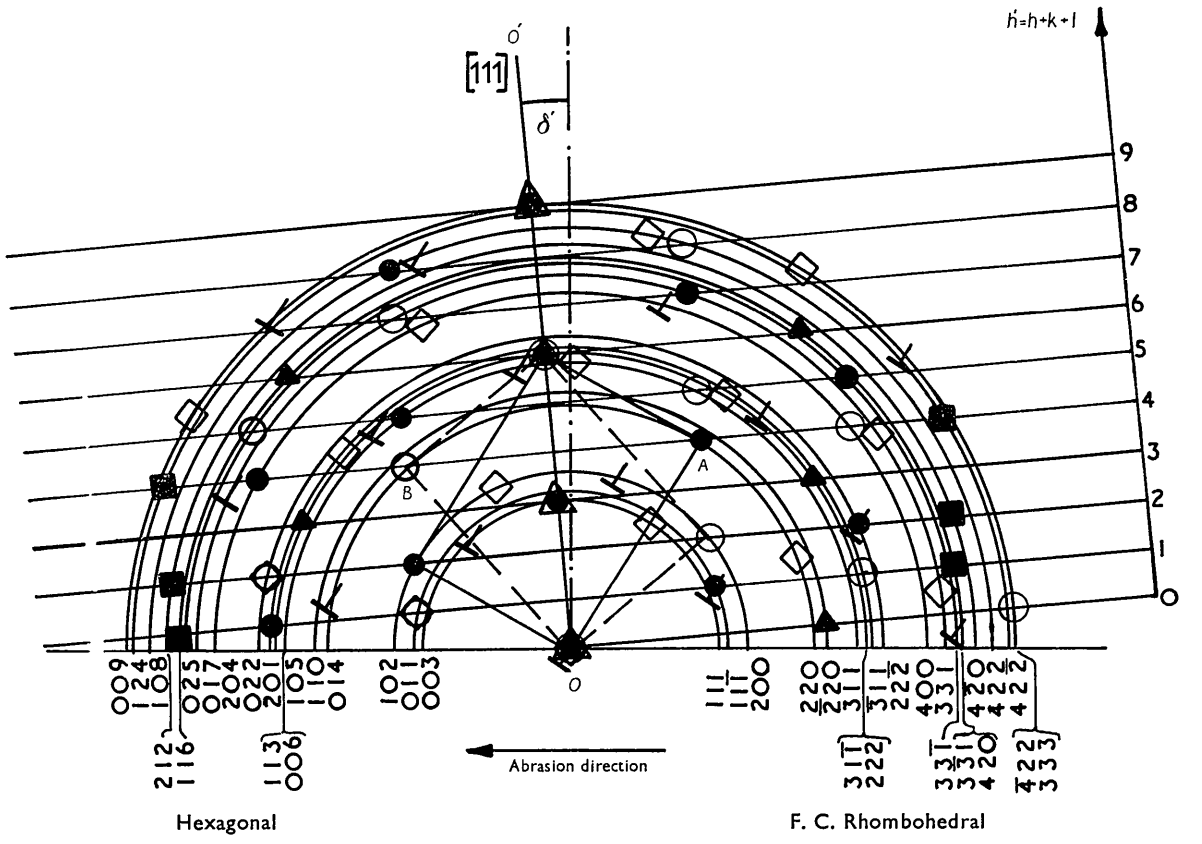

Fig. 4. Theoretical diffraction positions for antimony in one-degree orientation about a forwardly-inclined [111] axis OO'. ◇ and ✕ denote main sets of diffractions from pseudo-octahedral twins.

Patterns mainly similar to Fig. 2 were also obtained from the surfaces exposed by etching in further stages down to about 1·25 microns depth, below which the patterns became increasingly similar to Fig. 1, showing the undistorted original texture. Patterns such as Fig. 3(*a*) were obtained with the beam normal to the abrasion direction, after etching to a total depth of about 7500 Å. Fig. 3(*a*) is mainly closely similar (except for the left-hand 200 arc; see § 3(*d*)) to Fig. 2(*a*) but with shorter arcs indicating a narrower spread of orientation from the mean.

(*c*) *Evidence of an azimuthal range of orientation about a forwardly tilted* [111] *axis*

Figs. 2(*a*) and 3(*a*) are closely similar in the positions of the main strong arcs, which correspond, as Fig. 4 shows (the diffractions denoted by ●, ○, ▲ and ■), to an extensive azimuthal rotational range about the [111] axis *OO'* (f.c.rh. axes), which is inclined forward from the specimen normal (to the left in Figs. 2(*a*), 3(*a*) and 4), by an angle δ' which is about 10–12° in Fig. 2(*a*) and 1–2° in Fig. 3(*a*). (Note that Fig. 4 is not to the same scale as Figs. 2 and 3). The variation of δ' (and also δ, see § 3(*d*)) with depth below the abraded surface is shown in Fig. 7.

In Figs. 2(*a*) and 3(*a*) the set of arcs denoted by filled-in circles in Fig. 4, forming a centred pseudo-$\sqrt{2}$-rectangle array, is strongest. This represents an azimuthal orientation with a $\langle 1\bar{1}0\rangle$ type of lattice row parallel to the specimen surface and normal to the abrasion direction; but this orientation is concluded to be near, but not actually at, the mean of the preferred azimuthal range present (concerning which, see below). The set denoted by the open circles in Fig. 4 is less strong, though still of medium intensity; and it corresponds to an azimuth either 60° away, or 180° (equivalent to the twin on the nearly horizontal (111) plane), about the above [111] axis *OO'*. It seems likely that this set of arcs corresponds to an actual mechanical twinning of the antimony on these nearly horizontal (111) planes, rather than merely to an azimuthal spread of more than 60° from the above main preferred azimuth. This can be seen from the considerable intensity of this set of arcs compared with that of the arcs denoted by the triangles in Fig. 4 (in nearly $\sqrt{(8/3)}$-rectangle array), which correspond to a 30° azimuth orientation. Additional arcs present in Fig. 3(*a*) as compared with Fig. 2(*a*) also appear to indicate twinning on other pseudo-octahedral planes (see below).

It is also noticeable that in Fig. 2(*a*) the set of arcs

corresponding to the open circles in Fig. 4 is rotated as a whole by a few degrees in an anticlockwise direction, away from the positions shown in Fig. 4. In Fig. 3(*a*) the displacement is much smaller. This variation of δ' as a function of azimuth presumably corresponds to the different effects of the stresses upon these two symmetrically related lattice orientations during their development.

In Fig. 2(*b*), obtained with the electron beam in an azimuth 30° from that of Fig. 2(*a*), the relative positions of the arcs have not changed much from those of Fig. 2(*a*), but the relative intensities have changed. This, and Figs. 2(*c*) and 2(*d*) at other azimuths, confirm the marked azimuthal preference concluded above, of the orientation about the orientation axis. Fig. 2(*d*) shows that there is only about $\pm 30°$ spread of the orientation about the abrasion direction.

(*d*) *Interpretation of additional diffractions not corresponding to the* [111] *orientation*

While the above rotational spread in azimuth round the forwardly inclined [111] axis OO' is strongly analogous to that about the forwardly inclined [0001] orientation axis observed on abraded zinc and cadmium (Avient, 1961), there are certain diffraction arcs in Figs. 2(*a*) and 3(*a*) which are additional to those accounted for by Fig. 4. The positions of these arcs agree well with those of diffractions which would be produced (see Fig. 5) by a rotational range about the backwardly-inclined (110)-plane-normal OA, which corresponds in direction to OA of Fig. 4, tilted back by an angle δ from the specimen normal, such that $\delta + \delta' \simeq 38°$.

Such a backwardly inclined (110) orientation was observed to be produced by abrasion on f.c. cubic metals, with an azimuthal preference analogous to that of the rolling texture, *i.e.* with a $\langle 1\bar{1}2 \rangle$ type of direction (in the (110) plane) lying in the vertical plane through the abrasion direction (Goddard, Harker & Wilman, 1962). Crystals with the above orientation give rise to a hexagonal array of strong diffraction arcs (the innermost lying on the 220 ring position), when the beam is normal to the abrasion direction, *i.e.* along a cube diagonal. An azimuthal spread of more than $\pm 36°$ about the [110] axis,

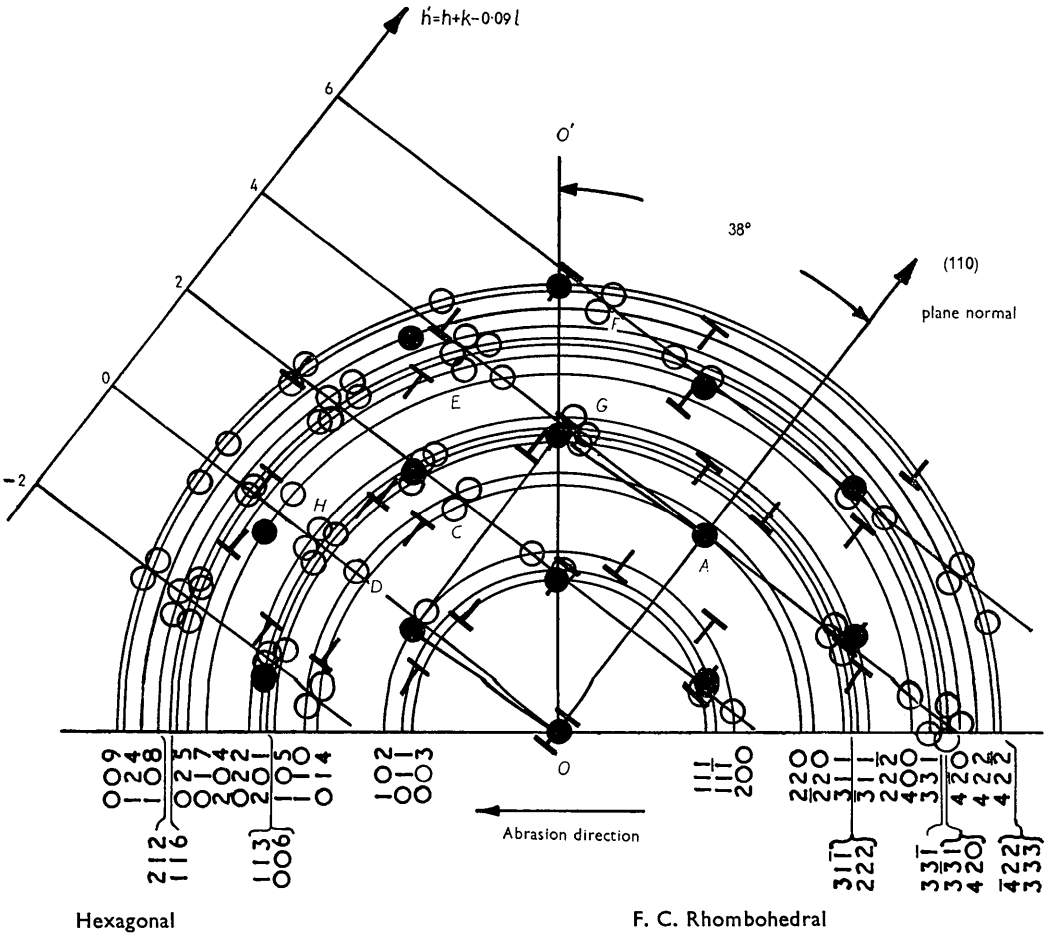

Fig. 5. Theoretical diffraction positions (○, ●) for antimony in one-degree orientation about a backwardly-inclined (110) plane normal. ✕ and ✕ denote main sets of diffractions from pseudo-octahedral twins.

from the above $\langle 1\bar{1}2\rangle$ preferred azimuth, results in the simultaneous appearance of strong diffractions forming a centred $\sqrt{2}$-rectangle array, also present in the patterns.

In the present case of the antimony, the indication is that the basic orientation is of the backwardly tilted (110) type, with $\langle 1\bar{1}2\rangle$ as the preferred azimuth in the vertical plane through the abrasion direction (analogous to that observed in the f.c. cubic metals). This can be seen from the following details in Figs. 2(*a*) and 3(*a*): (i) the primary pattern from the main preferred azimuth ($\langle 1\bar{1}2\rangle$ type of direction) is a pseudo-hexagonal array of diffractions which is indeed present, represented by the strong arcs denoted by *A* and *C* on the 220 ring position and *F* on the 422 ring position in Fig. 5, the radii to the first two enclosing an angle of 62° in agreement with the theoretical positions shown in Fig. 5; (ii) the prominent pseudo-$\sqrt{2}$-rectangle array of diffractions (filled in circles in Figs. 5 and 4) occurs as a result of the $> \pm 36°$ azimuthal spread of the (110) orientation; (iii) the $2\bar{2}0$ type of arc (*D* in Fig. 5) is centred on nearly the same radius as the left-hand strong 200 arc (*cf.* Figs. 2(*a*) and 3(*a*); (iv) a strong 331 type of arc is observed in Fig. 2(*a*), corresponding to the diffraction E slightly to the left of *OO'* in Fig. 5, whereas that contributed in this region from the forwardly inclined $\langle 111\rangle$ orientation (*cf.* Fig. 4) is further to the left, especially in view of the additional forward (anticlockwise) displacement of the set of diffractions denoted by the open circles in Fig. 4 (see above); (v) a $22\bar{2}$ arc is observed in Fig. 3(*a*) (less clearly in Fig. 2(*a*)) close to the arc *G* in Fig. 5. (This could also be due to presence of some $\{11\bar{1}\}$ orientation, *i.e.* with a $\{11\bar{1}\}$ plane-normal as axis, lying nearly along *OO'*, see Fig. 6); (vi) a $22\bar{2}$ arc is observed (most clearly in Fig. 3(*a*)) in the position *H* in Fig. 5, in addition to the slightly stronger $22\bar{2}$ arc below *H* and denoted by *T* in Fig. 5.

Fig. 3(*a*) shows, as compared with Fig. 2(*a*), a very prominent extension of the left hand 200 arc (and its higher order 400) towards the plane of incidence. This extension seems to be in about the position at which a 200 diffraction would be expected (denoted by a square in Fig. 4) if a $\{111\}$ twin had occurred of the antimony lattice corresponding to the open-circle set of diffractions in Fig. 4. The latter is itself in a $\{111\}$ twin relationship to the main lattice which corresponds to the filled-in circles in Fig. 4 (*cf.* § 3(*c*)). This might thus be evidence of secondary $\{111\}$ twinning. The other diffractions denoted by ◇ in Fig. 4 mostly coalesce with diffraction arcs already accounted for (see above and under (*c*)), and thus unfortunately cannot be distinguished to provide

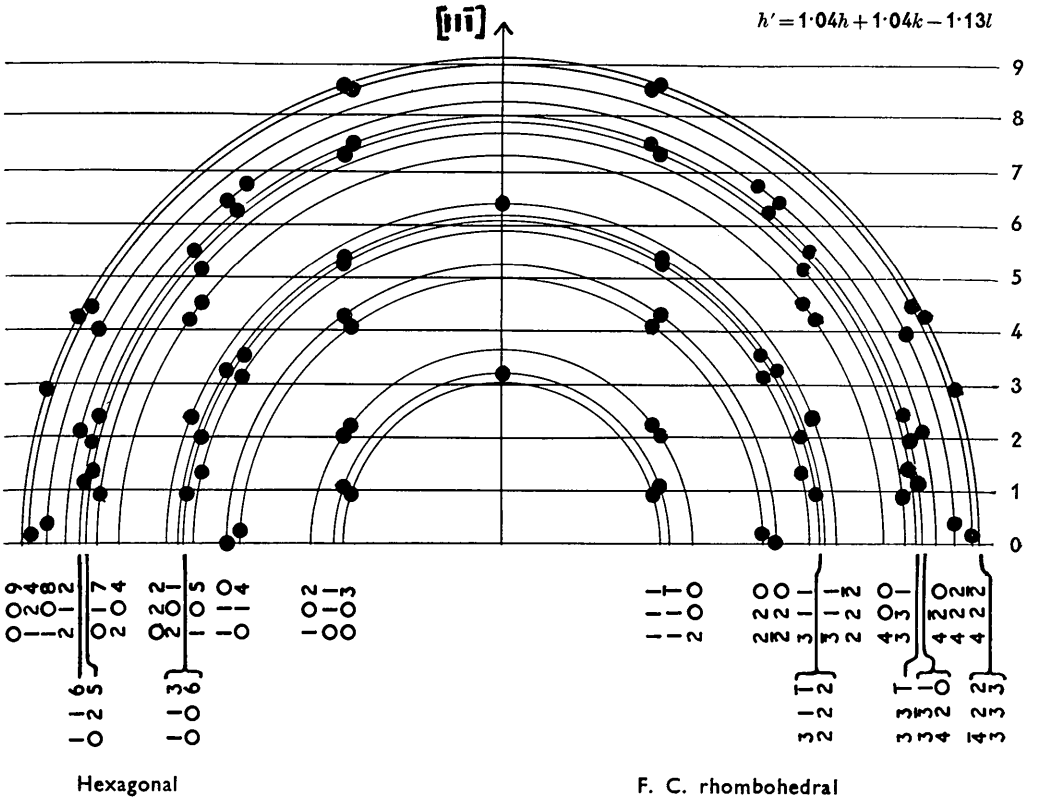

Fig. 6. Theoretical diffraction positions for Sb in one-degree orientation about a vertical $\{11\bar{1}\}$-plane normal.

further evidence in confirmation of this twinning. This prominent 200 arc extension (or coalescent pair of 200 arcs?) was observed at a similar stage of etching in observations on another antimony specimen also.

4. Discussion

The above results show clearly the nature of the 'abrasion texture' of antimony, *i.e.* the preferred orientation which is developed in the surface regions by unidirectional abrasion. This orientation is particularly interesting in its close relationship to the abrasion texture which we have found previously on f.c. cubic metals on the one hand, and on the hexagonal metals on the other hand, especially zinc and cadmium.

The evidence suggests that the antimony, which deviates only slightly from a f.c. cubic structure ($\alpha_{fr}=87°\ 25\ 4'$), develops, as a primary stage of the deformation in the abrasion, a preference for a backwardly inclined orientation of (110) type (f.c.rh. axes). The observed tilt δ of this orientation axis increases with depth below the abraded surface (Fig. 7), and reaches a value about equal to $\tan^{-1}\mu_{\text{emery, Sb}}$, *i.e.* the true mean coefficient of friction of the emery particles ploughing along the antimony.

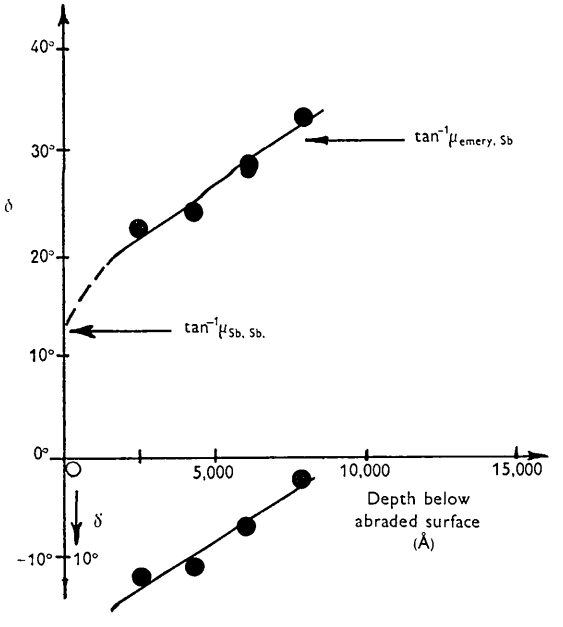

Fig. 7. The variation of the tilt δ of the backwardly-inclined orientation axis ((110) plane normal), and δ' of the forwardly-inclined [111] axis, with depth below the abraded Sb surface.

Although the extent of the azimuthal spread from the mean, together with the presence of a pair of symmetrically disposed equivalent azimuthal orientations, precludes definition of the exact mean of each azimuthal preference, it seems likely from the data that it is in fact such that a $\langle 1\bar{1}2\rangle$ direction (in the (110) plane) lies in the plane that is normal to the specimen surface and parallel to the abrasion direction. This inclined $\{110\}\langle 1\bar{1}2\rangle$ abrasion texture is the same as that found for the f.c. cubic metals (Goddard, Harker & Wilman, 1962), the tilt of the $\sim\langle 110\rangle$ orientation axis being backward from the specimen normal in the same way as for those metals.

Although this texture is suggested as occurring as a primary stage of the deformation during the abrasion, the evidence shows clearly, however, that in those crystals of this range which have a (111) plane parallel to the specimen surface or nearly so, there is a secondary stage of extensive azimuthal rotational spread about the slightly forwardly tilted (111) plane normal. Its azimuthal spread is at least $\pm 30°$ and either extends strongly to $\pm 60°$ or else that azimuth appears strongly as a result of pseudo-octahedral twinning. Such a rotational spread round the (111) slip-plane normal could be due to rotational slip (Wilman, 1950, 1951; Whapham, 1955; Whapham & Wilman, 1956) on these densely-populated planes. The above primary rotational spread about the $\{110\}$ plane normal appears to be present in part of the metal re-orientated by abrasion and this would further account for the right-hand 200 arc in Fig. 2(*b*) being still strong as compared with its intensity in Fig. 2(*a*), while the left-hand 200 arc in Fig. 2(*b*) is much weaker than in Fig. 2(*a*).

The above-described extensive rotation about the forwardly tilted [111] axis is strikingly analogous to the [0001] forwardly tilted abrasion texture observed to be produced in zinc and cadmium (Avient, 1961; Avient & Wilman, 1965) which is again practically identical with their rolling texture. Although Barrett (1953) refers to this rolling texture as being compatible with the dimension changes made during rolling, and involving much twinning, its origin seems to be somewhat obscure. The present results appear to account for the forward inclination of the antimony trigonal axis and its magnitude. They further suggest the possibility that zinc and cadmium may tend to become f.c. rhombohedral (pseudo-f.c. cubic) in structure temporarily during the actual deformation, reverting to hexagonal structure again on cessation of the deformation.

In the somewhat analogous case of graphite ($c/a=2{\cdot}726$), which is normally hexagonal, abrasion and grinding are known to result in formation of a considerable amount of the metastable rhombohedral form which is similar to the f.c. cubic lattice in the stacking of the (0001) layers of atoms. The easy slip of zinc and cadmium on (0001) could presumably similarly result in some layer sequence corresponding to rhombohedral stacking of these atom layers, even if such stacking reverted by dislocation movements (as in polygonization) to the hexagonal stacking. The heat liberation accompanying the abrasion would facilitate rapid dislocation movement and recrystallization to the normal hexagonal state.

The similarity of the behaviour of antimony to that of zinc and cadmium is associated similarly with a markedly higher spacing of the antimony (111) planes which are normal to the trigonal axis, than would correspond to close packing of spheres. For the hexagonal packing of spheres, $c/a = 1{\cdot}633$, whereas for antimony the equivalent ratio is 1·744, and this is about half way between 1·633 and the c/a of zinc and cadmium, *i.e.* 1·856 and 1·886 at 25 °C (Wyckoff, 1948) respectively.

The pseudo-octahedral twinning (submicroscopic) indicated strongly in the present results is a further expression of the pseudo-cubic form of the antimony structure, and does not appear to have been previously observed. The strong twinning (and secondary twinning) hitherto observed, presumably by optical means, has been identified as of {110} type relative to the f.c. rhombohedral pseudo-cubic axes (Gough & Cox, 1930, 1932; Hall, 1954). Since the deviation from f.c. cubic form is so slight, and since {110} is a plane of symmetry for a cubic lattice, such {110} twinning would only cause a few degrees change in lattice orientation, and this, together with the length of the observed diffraction arcs, may be why we did not observe clearly any twinning of this type, although some might have been present.

The above work was carried out under the terms of an extramural contract between the National Engineering Laboratory and the Imperial College of Science and Technology, University of London.

References

AVIENT, B. W. E. (1961). Ph.D. Thesis, Univ. of London.

AVIENT, B. W. E. & WILMAN, H. (1965). *Acta Cryst.* To be published.

BARRETT, C. S. (1953). *The Structure of Metals.* London and New York: McGraw-Hill.

CUCKA, P. & BARRETT, C. S. (1962). *Acta Cryst.* **15**, 865.

DOBSON, P. S. & WILMAN, H. (1962*a*). *Acta Cryst.* **15**, 794.

DOBSON, P. S. & WILMAN, H. (1962*b*). *Acta Cryst.* **15**, 800.

FINCH, G. I. & WILMAN, H. (1937). *Ergebn. exakt. Naturwiss*, **16**, 353.

GODDARD, J., HARKER, H. J. & WILMAN, H. (1962). *Proc. Phys. Soc.* **80**, 771.

GOUGH, H. J. & COX. H. L. (1930). *Proc. Roy. Soc.* A, **127**, 431.

GOUGH, H. J. & COX, H. L. (1932). *J. Inst. Metals*, **48**, 227.

HALL, E. O. (1954). *Twinning and Diffusionless Transformations in Metals.* London: Butterworths.

KING, J. N. & WILMAN, H. (1961). *Proc. Phys. Soc.* **78**, 979.

KING, J. N. & WILMAN, H. (1962). *Wear*, **5**, 213.

LEVIN, P. H. (1960). Ph.D. Thesis. Univ. of London.

SCOTT, V. D. & WILMAN, H. (1958). *Proc. Roy. Soc. A*, **247**, 353.

STROUD, M. F. & WILMAN, H. (1963). *Brit. J. Appl. Phys.* **14**, 381.

WYCKOFF, R. W. G. (1948). *Crystal Structures.* London and New York: Interscience.

WHAPHAM, A. D. (1955). *J. Inst. Metals*, **84**, 109.

WHAPHAM, A. D. & WILMAN, H. (1956). *Proc. Roy. Soc.* A, **237**, 513.

WILMAN, H. (1950). *Nature, Lond.* **165**, 321.

WILMAN, H. (1951). *Proc. Phys. Soc.* A, **64**, 329.

Acta Cryst. (1965). **18**, 449

The Crystal Structure of Decammine-μ-peroxodicobalt Tetrathiocyanate

BY NILS-GÖSTA VANNERBERG

Department of Inorganic Chemistry, Chalmers University of Technology and University of Gothenburg, Sweden

(*Received* 10 *April* 1964)

The compound $[(NH_3)_5CoO_2Co(NH_3)_5](SCN)_4$ has been prepared and its structure determined. The space group is *Pnnm* No. 58, with $a = 13{\cdot}22$, $b = 10{\cdot}58$, $c = 7{\cdot}88$ Å. The two cobalt atoms are linked together by a peroxide group, each cobalt atom being bonded to one oxygen atom.

Introduction

Cobalt forms two kinds of μ-peroxo complex ions, *viz.* $[(NH_3)_5CoO_2Co(NH_3)_5]^{5+}$ and $[(NH_3)_5CoO_2Co(NH_3)_5]^{4+}$. The structure of the former was determined and described by Vannerberg & Brosset (1963). In that paper was also given a historical introduction to the subject. In this paper the structure of decammine-μ-peroxodicobalt(III) tetrathiocyanate will be described.

Experimental and crystal data

Very well developed needle-shaped crystals of decammine-μ-peroxodicobalt(III) tetrathiocyanate are formed when a strongly ammoniacal solution of cobalt(II) thiocyanate is allowed to stand in contact with air. (Analysis: Found: Co 20·6, NH_3 30·0, SCN 41·7%. Calculated: Co 21·3, NH_3 30·8, SCN 42·1%.) The crystals have orthorhombic symmetry. The unit cell